

CHAPTER 78

Periodic Flows from Tidal Inlets

by D.L. Wilkinson *

Introduction

A study was undertaken of the flow produced in the offshore region by tidal currents at the entrance of a coastal inlet. The gross features of the offshore flow structure were examined in an idealised two dimensional model in which a sinusoidally reversing flow was discharged from an open channel into a large stagnant basin. During each period of ebb flow, the discharge from the simulated inlet developed a structure very similar to that of a starting jet, and a vortex pair was observed to form and ultimately became the dominant feature of the flow. Although variable bottom topography and long shore currents will distort the flow pattern, the rotational motions observed in these experiments would be expected to persist.

The study was restricted to coastal inlets in which the sectional area of the entrance channel is several orders of magnitude smaller than the area of water surface inside the inlet.

Length and Time Scales of the Flow

The flow under study is shown schematically in Figure 1.

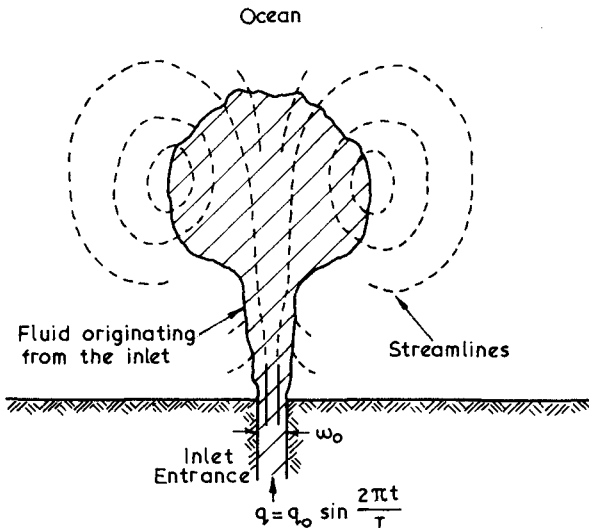


Figure 1: Schematic diagram of outflow from inlet

* Senior Lecturer, The University of New South Wales, Australia.

A periodically reversing flow passed through the entrance channel which joins to a large basin. The depths in the basin and the channel are uniform and the same. The flow per unit depth Q varies with time t according to the relationship

$$Q = Q_0 \sin \frac{2 \pi t}{T} \tag{1}$$

where Q_0 is the maximum flow rate and T is the tidal period.

It is well known that steady jets conserve axial momentum and that no characteristic length scale can be ascribed to them. However, if the strength of the jet is periodic with period T , it can be readily shown that a characteristic length scale exists for the motion. A periodic two dimensional jet at high Reynolds Numbers is fully defined by m_0 the maximum value of the momentum eflux, the period T , the width of the entrance channel w_0 , and the fluid density ρ . The momentum flux m_0 is given by

$$m_0 = \frac{\rho Q_0^2}{w_0} \tag{2}$$

The variables m_0 , T and ρ can be combined to give a characteristic length l which is now defined as

$$l = \left(\frac{1}{\rho} m_0 T^2 \right)^{1/3} \tag{3}$$

This is the appropriate length scale by which the structure of the flow may be described. Experiments have shown that l is of the order of the jet size, one period after the commencement of the ebb flow.

Any other flow parameter, for example the breadth b of the jet, at time t and distance x from the entrance, can be expressed non-dimensionally as

$$\frac{b}{l} = \text{fn} \left(\frac{x}{l}, \tau, \frac{w_0}{l} \right) \tag{4}$$

where τ is the normalised time t/T .

It is well established that the structure of steady jets is independent of the initial velocity structure at distances of 20 or more source widths downstream of the discharge point. Turbulence resulting from Kelvin-Helmholtz type instability in the shear zone, spreads in a direction normal to flow and destroys any initial structure. A similar situation can be expected to exist in the periodic jet provided the dimensions of the inlet are small compared with the size of the flow structures which develop. That is the ratio w_0/l must be small. This being so, it can be expected that periodic jets will have a general structural similarity at similar non-dimensional times.

Experiments

Experiments were conducted with three aims in mind:

- (i) To examine the basic structure of the flow and to check that the characteristic length as defined in Equation (3) was the appropriate scaling parameter.
- (ii) To examine the significance of the entrance width ratio on the normalised flow structure.
- (iii) To determine the proportion of the flow which returns to the inlet having been discharged on the previous ebb tide.

The experiments were performed in a tank 5m square and filled to a depth of approximately 100mm. The width of the entrance channel ranged from 25mm to 97mm and the maximum tidal velocities ranged from 30mm s^{-1} to 110mm s^{-1} in the different experiments. Reynold's numbers in the entrance were never less than 4000 at peak outflow. The periodic flow was achieved using the system shown in Figure 2.

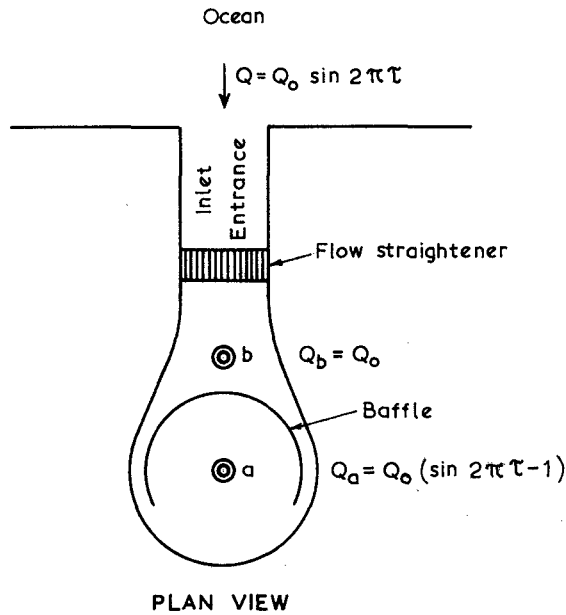


Figure 2: Periodic flow generator

A constant flow Q_0 was discharged through a vertical manifold at b. A flow Q_a was drained from a location a and this flow was regulated by means of a motor driven valve to produce the flow $Q_a = Q_0(\sin 2\pi\tau - 1)$, that is, the withdrawn flow varied sinusoidally between 0 and $2Q_0$. The difference between the flows at a and b discharged into the model ocean and this flow varied sinusoidally between $-Q_0$ and $+Q_0$. The

tidal period used in the experiments was constant at 60s.

It will be noted with this system geometry, the ebb flow can only originate from Q_b and this flow was tabled with a very weak electrolyte solution so that concentrations of water originating from the inlet could be monitored in the ocean by means of conductivity probes. The addition of the electrolyte produced no detectable density stratification in any part of the model.

Structure of the Flow

The photographs in Figure 3 show the structure of the flow at dimensionless times $\tau = 0.25, 0.50, 0.75$ and 1.06 corresponding to

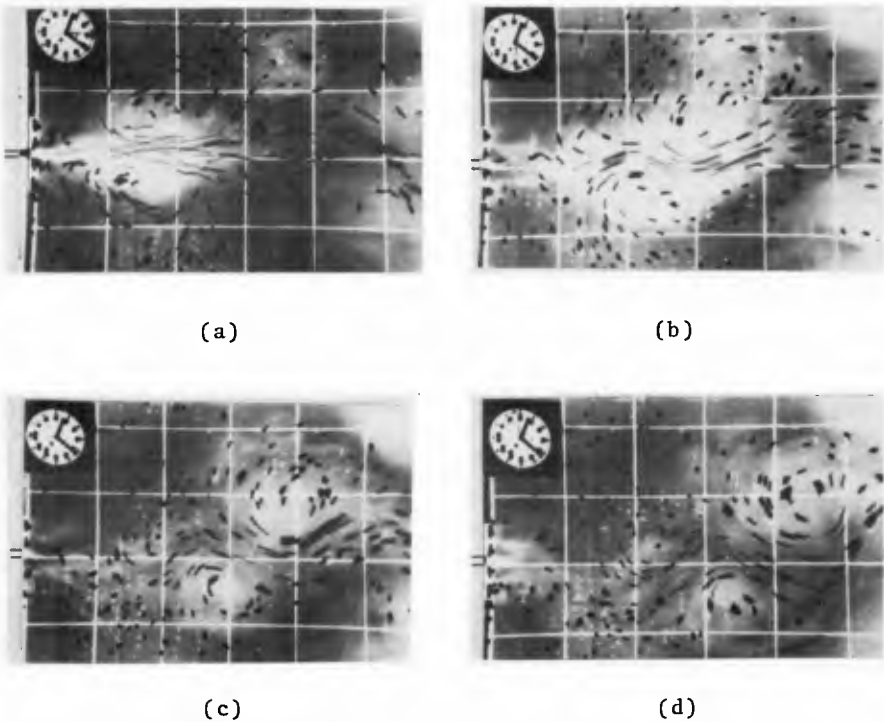


Figure 3: Structure of the flow at various phases

maximum ebb flow, low slack water, maximum flood flow and shortly after high slack water. The structure is revealed by means of streaklines observed by a stationary camera exposed for a time $\tau = 0.03$ (2 seconds). Water originating from the inlet was dyed in these experiments and shows as lighter coloured areas in the photo-

graphs. The grid scale consists of 200mm squares.

The entrance width ratio in this experiment was $w_0/l = 0.02$ which may be considered as small. The first photograph (a) shows the flow when the ebb current in the entrance is a maximum. It will be seen that a vortex pair has formed and is symmetrically placed about the entrance channel. Note that most of the circulation at this stage involves ocean fluid and is uncontaminated with water discharged from the inlet. This implies that the vortical motion is largely irrotational since vorticity can only be introduced from the shear layers at the boundary of the jet.

As time progresses, each vortex is spun up at a rate equal to the moment of momentum of the half jet and in photograph (b) taken at low slack water it will be observed that the areal extent of the vortices has increased and because of their mutual interaction they have moved further away from the entrance. Note also that because of the interaction, velocities are a maximum midway between the two vortices and that the symmetry observed in the previous photograph is no longer apparent. This results from the interaction of the present vortex pair with pairs formed during previous tidal cycles. In photograph (c), taken at maximum flood flow, the vortices are so distant from the entrance that the flow reversal has minimal effect on their motion. It can also be seen that the major portion of the fluid discharged from the inlet on the ebb cycle is now contained within the vortices which continue to move seawards. Photograph d was taken just after high slack water. The new ebb flow has just commenced to flow from the entrance and the vortices from the previous cycle are still clearly visible.

Profiles of the dyed inlet fluid normalised with respect to the characteristic length are shown at several stages of the tide in Figure 4. The physical value of the length scale was different in each of these experiments and the collapse of the data confirms that the scale formulation of Equation (3) is valid. Furthermore, the value of the inlet width ratio in each of these experiments was different but always less than 0.05. This suggests that like steady jets, the structure of periodic jets is independent of the entrance conditions provided the characteristic length of the flow is large compared with the dimensions of the entrance.

Figure 5 shows the normalised velocity structure of the flow at various tidal phases. The velocity maxima was found to always occur between the two vortices, and the distribution of the axial velocity component along a line joining the centres of the vortices at time $\tau = 0.5$ suggests that the flow could be modelled by a pair of interacting Rankine vortices.

It is not evident in the photographs; however, on the flood tide, the flow into the entrance was found to be very similar to that predicted

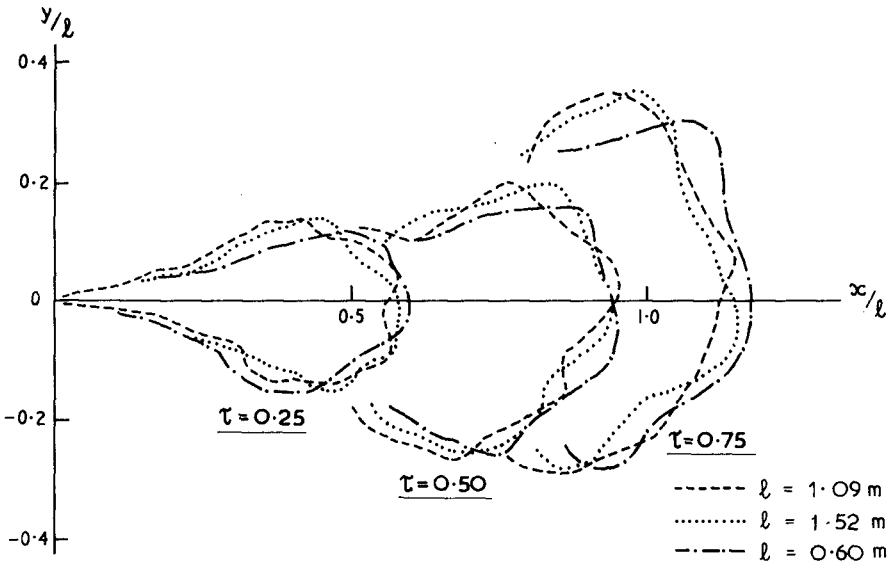


Figure 4: Normalised flow profiles for small values of $w_0/1$

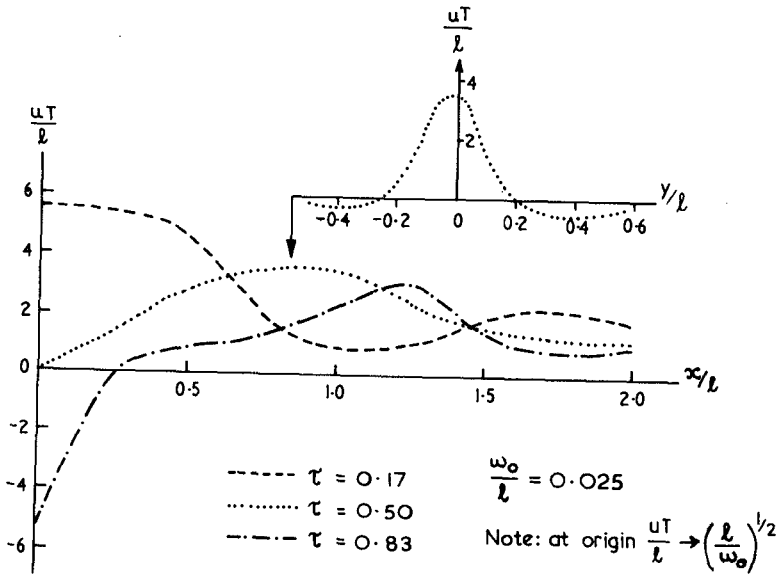


Figure 5: Normalised velocity profiles of ebb flow

by potential flow theory. The flow was radially uniformly distributed about the entrance, and consequently the ocean area affected by the flood tide was very much less than that affected by the ebb tide.

Significance of the Inlet Width Ratio

It has been shown that provided the inlet width ratio is small (less than approximately 0.05), the structure of periodic jets is similar at any given value of the tidal phase. It remains to determine how valid this condition will be in real inlets. It is well established in many tidal inlets that the sectional area of the entrance channel, A , is in almost linear proportion to the mean tidal prism, P (O'Brien 1931). The constant of proportionality in the relationship is found to have a value of approximately $6 \times 10^{-5} \text{ m}^{-1}$ so that

$$A = 6 \times 10^{-5} P \quad (5)$$

In terms of the two dimensional model

$$\begin{aligned} A &\doteq w_0 \\ \text{and } P &\doteq \int_0^{T/2} Q \, dt = \frac{Q_0 T}{\pi} \end{aligned} \quad (6)$$

However, Equations (2) and (3) give

$$Q_0 T = (w_0 l^3)^{1/2} \quad (7)$$

which on substituting into Equation (5) gives

$$\begin{aligned} w_0 &= \frac{6 \times 10^{-5}}{\pi} (w_0 l^3)^{1/2} \\ \text{or } \frac{w_0}{l} &= 4 \times 10^{-10} l^2 \end{aligned} \quad (8)$$

Hence the entrance ratio can only be considered small for inlets with characteristic lengths of approximately 10km or less. This corresponds to tidal prisms of up to a maximum of $2 \times 10^7 \text{ km}^3$ where d is the mean depth of the entrance channel.

The effect of increased entrance width ratio can be seen in Figure 6 where normalised ebb profiles, as defined by dyed fluid emerging from the inlet, are shown for w_0/l ratios of 0.02 and 0.15 at dimensionless times $\tau = 0.25, 0.50$ and 0.75 . The breadth of the ebb discharge is appreciably greater for flows having higher entrance width ratios and this is particularly true in the immediate vicinity of the entrance channel. Therefore it is to be expected that the fraction of water returning to the inlet on the flood tide will increase as the entrance width ratio increases in value.

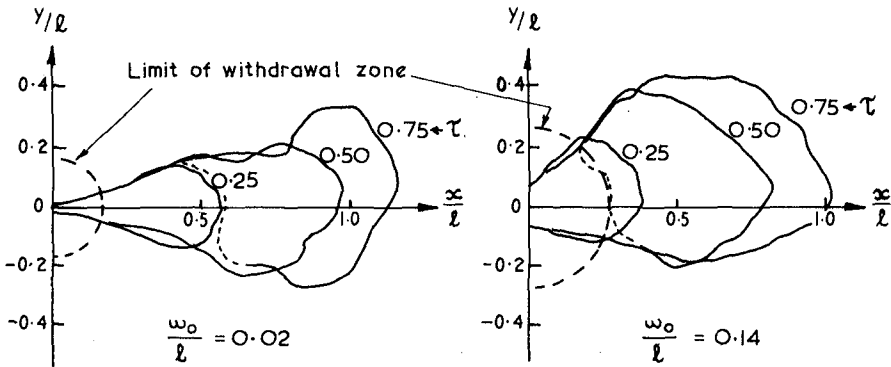


Figure 6: Effect of entrance width on the flow profiles

A further effect reinforces the above trend. The tidal prism P can be used to define a radius of withdrawal R at the channel entrance so that

$$\frac{\pi R^2}{2} = P \tag{9}$$

However, the tidal prism can be expressed in terms of l via Equations (6) and (7) to give

$$\frac{R}{l} = \frac{\sqrt{2}}{\pi} \left(\frac{w_0}{l} \right)^{\frac{1}{4}} \tag{10}$$

Thus the extent of the withdrawal zone increases as the entrance width ratio increases. The limits of the withdrawal regions for the two experiments shown in Figure 6 are indicated by the semi-circles encompassing the entrances.

It is apparent in Figure 6 that the fraction of water which returns to the inlet on the flood tide, having been discharged on the preceding ebb, will increase as the entrance width ratio of the inlet increases. This trend is clearly shown in Figure 7 where the fraction of returning water in the flood flow is plotted against tidal phase. These data were obtained by means of conductivity probes located in the entrance channel which detected the concentration of electrolyte labeled fluid in the incoming flow.

The flushing capacity of an inlet reduced as the entrance width ratio of the inlet increased. This is clearly demonstrated in Figure 8 which shows the fraction of water which returns to an inlet as a function of the entrance width ratio of the inlet. Equation (8) indicates that the flushing ability will reduce as the tidal prism increases for inlets con-

forming to the O'Brien relationship.

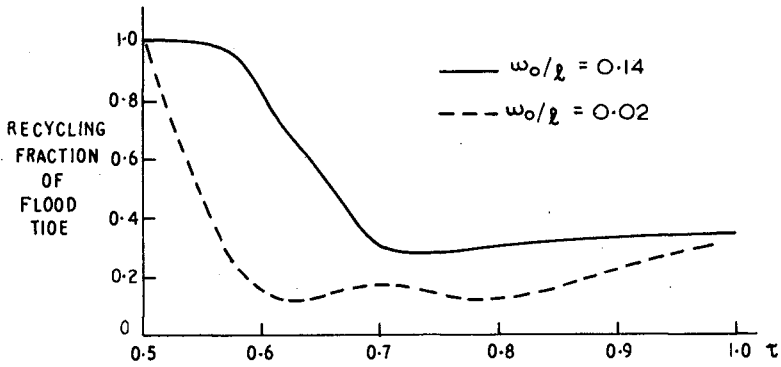


Figure 7: Fraction of water recycling on flood tide as a function of tidal phase

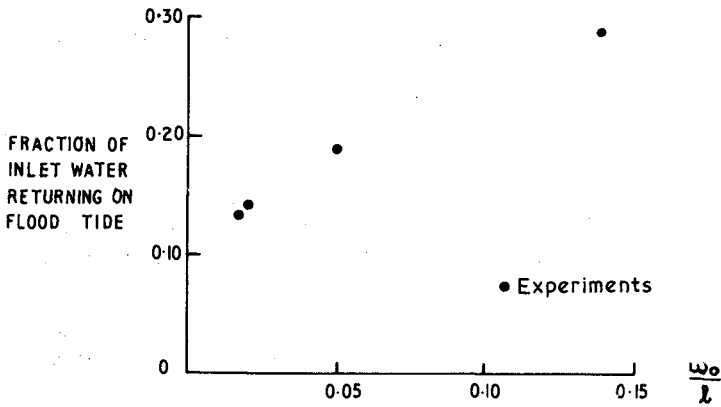


Figure 8: Fraction of inlet water returning on subsequent tide as a function of the entrance width ratio

Bottom Friction

It is to be expected that, in real estuaries, where the water depth would be relatively much less than in the experiments described here, the effect of bottom friction would be proportionately greater.

A measure of the importance of friction in real estuaries may be had by comparing the impulse (I), applied to the flow by bottom friction in one tidal period, with the total momentum M discharged from the inlet on the ebb tide. Thus

$$I = \int_0^T \int^A \frac{\rho g u^2}{C^2} dA dt$$

and
$$M = \int_0^{T/2} m d dt$$

in which C is the Chezy friction coefficient, A is the plan area of the flow associated with the discharge between times t = 0 and T = T, u is the axial velocity component within that area and d is the mean depth of the entrance channel.

Values of the impulse and total momentum can be expressed in terms of the characteristic variables, and the orders of magnitude of these two terms are

$$I = O \left[\frac{g}{10C^2} \left(\frac{1}{w_0} \right) \rho \frac{l^4}{T} \right]$$

and
$$M = O \left[\frac{d}{l} \frac{1}{w_0} \rho \frac{l^4}{T} \right]$$

Thus
$$\frac{I}{M} = O \left[\frac{g}{10C^2} \frac{1}{d} \right]$$

For a typical inlet in which

$$\frac{1}{d} = O [10^3]$$

and Chezy 'C' = 50 m^{1/2} s⁻¹

$$\frac{I}{M} = O [10^{-1} \text{ to } 1.0]$$

Thus substantial frictional effects could be expected in the prototype situation. These would be apparent in the far field (say for X/l > 0.5) where bottom friction will have done more work on the flow.

Conclusions

The off-shore flow structure at a tidal inlet resembles a starting jet during the period of ebb flow, and a potential flow during the flood half of the tidal cycle. The flow pattern is periodic and can be described non-dimensionally in terms of length and time scales based on the maximum value of the momentum flux emerging from the inlet and the tidal period.

The flushing capability of the inlet decreases as the normalised width of the entrance reduces in value.

Real inlets rarely conform to the idealised two dimensional conditions considered in this paper. Bottom friction will exert an appreciable influence on the flow particularly at distances of the order length scale. The offshore slope will also affect the motion tending to increase the angular speed of the vortices while diminishing their size. In spite of these influences, the basic structures observed in the experiments described here could be expected to persist in prototype situations.

Acknowledgements

The author would like to thank Mr. C.A. Miller for suggesting the means of obtaining the periodic flow and to Mr. R.B. Tomlinson for his assistance with the experiments.

Reference

O'Brien, M.P.: Estuary Tidal Prisms Related to Entrance Areas, J. Civ. Eng., 1 (8) pp 738-793 (1931).